Organic LETTERS

Letter

pubs.acs.org/OrgLett

Isomers of Pyrene–Imidazole Compounds: Synthesis and Configuration Effect on Optical Properties

Yulong Liu,[†] Tong Shan,[†] Liang Yao,[†] Qing Bai,[†] Yachen Guo,[†] Jinyu Li,[†] Xiao Han,[†] Weijun Li,[†] Zhiming Wang,[§] Bing Yang,[†] Ping Lu,*[,†] and Yuguang Ma[‡]

[†]State Key Laboratory of Supramolecular Structure and Materials, Jilin University, 2699 Qianjin Avenue, Changchun 130012, China

[‡]Institute of Polymer Optoelectronic Materials and Devices, State Key Laboratory of Luminescent Materials and Devices, South China University of Technology, Guangzhou 510640, China

[§]School of Petrochemical Engineering, Shenyang University of Technology, Liaoyang 111003, China

Supporting Information

ABSTRACT: Two pyrene-imidazole-based structural isomers, axisymmetric *syn*-PyDTI and centrosymmetric *anti*-PyDTI, have been easily produced and successfully separated in a one-pot reaction. Crystalline *syn*-PyDTI exhibited a 2-fold higher quantum efficiency than *anti*-PyDTI and displayed a much better performance in OLEDs with a $\eta_{c.max}$ of 11.4 cd A^{-1} (8.8 cd A^{-1} for *anti*-PyDTI), although they possess the same apparent electronic structure. Observations revealed that the molecular excited-state properties are derived from distinct structural symmetries.

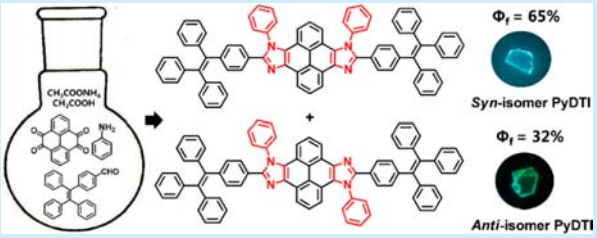

Isomers are one of the central issues in chemistry, especially for applications in medicinal[1,2] and materials sciences.[3,4] In the optoelectronics field, isomers have also attracted tremendous attention.[5] For instance, structural isomers, which contain the same bond structure but differ in the geometrical positions of their atoms in space, do not necessarily share similar properties, even if they have the same functional groups; thus, they can be utilized as valuable and model compounds to investigate the relationship between structure and properties.[6,7] A typical example involves the intensive study of the *syn*-/*anti*-isomeric effects on the critical changes of physical and optical properties of thiophene derivatives.[8−11] Pure *anti*-isomers exhibit much higher charge mobilities than their corresponding *syn*-counterparts in organic field effect transistors, and this phenomenon has been described by various groups for anthradithiophene, dicyanomethylenedithiophene, anthrabisbenzothiophene, and other systems.[9−11] One possible reason for this phenomenon may be attributable to the distinct dipole moments of *syn*-/*anti*-isomers. These valuable studies have significantly promoted the development of functional materials in optoelectronics and have contributed to the basic knowledge of isomers in organic chemistry.

In prior studies, *syn*-/*anti*-isomers have generally been synthesized independently through various synthetic routes.[8−12] It would be beneficial if these materials could be obtained via a one-step route and conveniently purified. In this paper, we demonstrate a strategy for achieving this goal and found a dramatic configuration effect on the optical property. 1,3-Imidazole is a commonly used, five-membered-ring functional group in efficient luminescent materials because of its amphoteric characteristics, which originate from the two types of sp^2 hybrid nitrogen atoms.[13−16] Pyrene has been one of the most important and thoroughly investigated organic chromophores in previous years.[17−19] Its 4, 5, 9, and 10 positions can be functionalized to yield periphery-modified pyrene-4,5,9,10-tetraones,[20] providing the opportunity to further create a polycyclic skeleton.[12,21] One of the insufficiently resolved issues involving the pyrene π-system is that it suffers heavily from aggregation-caused quenching that originates from the strong $\pi-\pi$ interaction between molecules.[22] To address this concern, the covalent bonding of an aggregation-induced emission (AIE)-active unit, such as tetraphenylethylene (TPE), has proved to be a powerful way to achieve high solid-state photoluminescence.[23] Based on this consideration, here, novel *syn*-/*anti*-structural isomers consisting of multiple functional groups, including pyrene (rigid π-structure), imidazole (nonsymmetrical units), and TPE (AIE block), are obtained in a one-pot reaction. Axisymmetric *syn*-PyDTI and centrosymmetric *anti*-PyDTI are readily formed during the synthesis process. These isomers are successfully separated with high purity. It is interesting to note that the *syn*-PyDTI exhibits 2-fold higher fluorescent quantum efficiency in the crystal and 1.5-fold higher quantum efficiency in evaporated amorphous film than that of *anti*-PyDTI, although they possess the same apparent electronic structure. The present findings can pave the way for the development of a new type of structural isomer and promotes the development of efficient organic luminescent materials that are regulated by molecular design.

Scheme 1 depicts the synthesis of the *syn*-isomer and the *anti*-isomer of PyDTI. These two compounds could be formed

Received: October 31, 2015
Published: December 7, 2015

DOI: 10.1021/acs.orglett.5b02879
Org. Lett. 2015, 17, 6138−6141

Scheme 1. Synthetic Approach to PyDTI Isomers

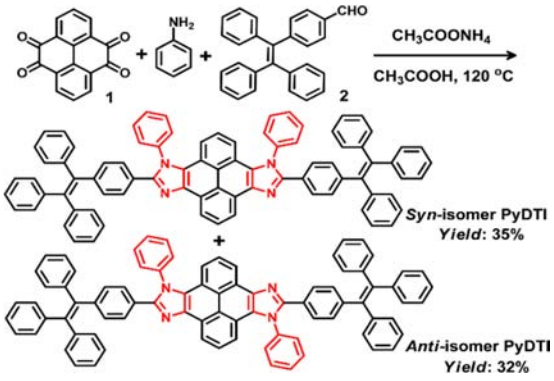

simultaneously via a "click-like" one-pot reaction.[21,24] The observed R_f values for these two isomers on a silica gel plate varied significantly when eluted with dichloromethane. This was a consequence of the various symmetries of the *syn*- and *anti*-isomers, which produced rigid polycyclic aromatic hydrocarbons with enhanced differences in molecular shape and polarity. Thus, the *syn*- and *anti*-PyDTI could be separated successfully by column chromatography in a nearly 1:1 ratio. In the ^{1}H NMR spectra (Figure 1), it can be seen that the

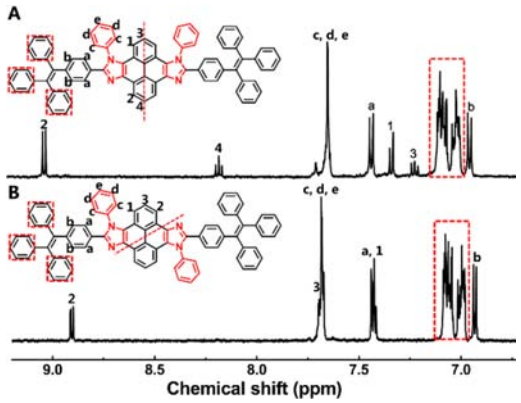

Figure 1. ^{1}H NMR spectra of *syn*-PyDTI (A) and *anti*-PyDTI (B) in C_4D_8O (500 M Hz, 298 K).

resonance peaks of protons H_1 and H_3 in *syn*-PyDTI occurred at 7.32 and 7.25 ppm, respectively, while those on the other side of the pyrene units, such as H_2 and H_4, displayed relatively low-field chemical shifts of 9.02 and 8.16 ppm, respectively. This difference could be a result of the fact that the ring-current effect,[25] which originated from two axisymmetric phenyl rings attached to the N atom, gave rise to a relatively strong shielding effect of protons H_1 and H_3, leading to a concomitant upfield chemical shift. In contrast, *anti*-PyDTI possessed a centrosymmetric structure, and the corresponding signals of the aromatic protons H_1 and H_3 presented a downfield shift at approximately 7.42 and 7.69 ppm. The characteristic ^{1}H NMR signals for both protons remained unchanged after UV irradiation. This indicated that photochemical isomerization could not occur in *syn*/*anti*-PyDTIs suggesting the good stability of these isomers.

The single-crystal measurement further confirmed the configuration of *syn*/*anti*-PyDTI. As depicted in Figure 2, both crystals belonged to the triclinic space group *P*-1. The *anti*-PyDTI crystal showed a centrosymmetric, coplanar

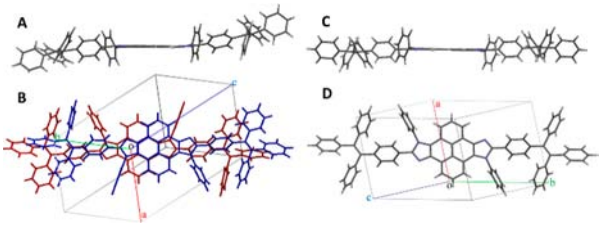

Figure 2. (A, C) Molecular structure side views of *syn*- and *anti*-PyDTI crystals. (B, D) Unit cell structure top views of crystalline *syn*- and *anti*-PyDTI.

configuration and a slip-stacked packing mode along the long molecular axis (Figure 2D and Figure S12-(2), Supporting Information). In contrast, *syn*-PyDTI manifested a clear twisted configuration (Figure 2A). Because the axisymmetric structure of *syn*-PyDTI would induce a dipole along the short axis direction (Figure S7 and Table S1, Supporting Information), it is proposed that the dipole−dipole interactions drove the formation of a flat dimer in one unit cell by alternating the antiparallel alignment[26] of the pyrene−imidazole unit with an interfacial distance of ∼4.0 Å (Figure 2B and Figure S12-(1), Supporting Information). The successful separation and confirmation of isomers is significant for achieving a deep understanding of the resulting optical properties at the molecular level.

Both isomers showed AIE activity. They were nonemissive in THF but exhibited intense emission in their aggregate states (Figure S10, Supporting Information). Comparing the crystals' emissions revealed a red-shift for the *anti*-isomer; that is, the *syn*-PyDTI crystal exhibited an emission peak at 465 nm, whereas the *anti*-isomer crystal displayed an emission peak at 507 nm (Figure 3A). The high-quality single crystals of *syn*- and

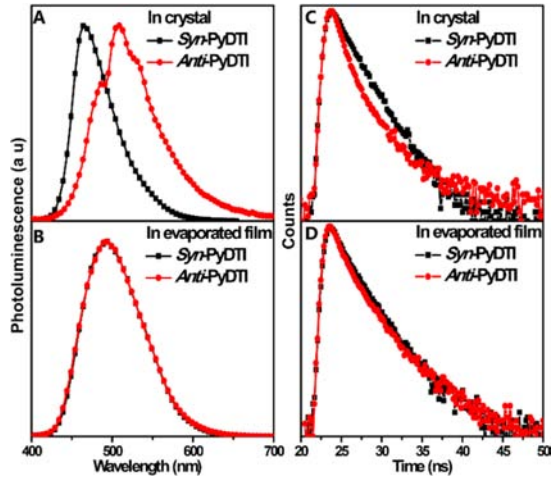

Figure 3. Emission spectra (A, B) and time-resolved peak fluorescence by time-correlated single-photon counting measurements (C, D) of *syn*-PyDTI and *anti*-PyDTI as crystals and evaporated films.

anti-PyDTI were blue and green under UV light, respectfully, which directly confirmed their different luminescent properties. As shown in their packing diagrams (Figure S12, Supporting Information), the intermolecular interactions were relatively small because of the large distance between the slip-packed adjacent molecules in *anti*-PyDTI, which would not significantly increase the effective conjugation length. The blue-shift observed in the *syn*-PyDTI crystal's emission spectrum was

DOI: 10.1021/acs.orglett.5b02879
Org. Lett. 2015, 17, 6138−6141

probably associated with the formation of dimers, which resulted in a flexible geometry and a decreased conjugation length. It can also be confirmed by their absorption spectra, where the initial band of *anti*-PyDTI was found at 438 nm and that of *syn*-PyDTI was located at 403 nm (Figure S9, Supporting Information). More importantly, the isomers manifested significantly different quantum efficiencies, as revealed by measurements obtained by an integrating sphere system. The efficiency of the *anti*-PyDTI crystal was calculated as 32%, while that for the *syn*-crystal was even higher to be 65%. In evaporated amorphous films, both species presented the same broad red-shifted emission spectra that peaked at 495 nm, indicating strengthened intermolecular interactions (Figure 3B). However, *syn*-PyDTI exhibited a quantum efficiency (φ_f) of 53%, which was higher than the *anti*-PyDTI efficiency of 35%.

In the excited state dynamics study, the nonradiative decay rate constant for the evaporated film of the *syn*-isomer was calculated to be 1.9×10^8 s^{-1}, which was much smaller than that of *anti*-PyDTI (3.1×10^8 s^{-1}). This indicates that the molecular vibrational modes of excited state of *syn*-PyDTI might effectively suppress the energy loss through nonradiative decay processes and afford a higher efficiency (Table 1). This

Table 1. Parameters for Exciton Dynamics in Crystals and Evaporated Films

	Φ_f[a]	τ (ns)	$k_r/10^8$[b] (s^{-1})	$k_{nr}/10^8$[b] (s^{-1})
syn-crystal	0.65	2.12	3.1	1.6
anti-crystal	0.32	1.66	1.9	4.1
syn-film	0.53	2.45	2.2	1.9
anti-film	0.35	2.10	1.7	3.1

[a]Measured by an integrating sphere system. [b]The radiative and nonradiative exciton decay rate constants k_r and k_{nr} can be calculated using equations S1−S4 in the Supporting Information.

type of situation was more obvious in the crystal because the time-resolved fluorescence spectroscopy of the *syn*-PyDTI crystal showed monoexponential decays from the excited singlet state. This behavior suggested that the fluorescence originated from only one excited state and that no competing radiative deactivation process existed (Figure 3C). Thus, the various symmetries characteristic of *syn*- and *anti*-isomers induced crucial changes in the photophysical propeties.

OLEDs were fabricated with the classical structure of ITO/PEDOT:PSS (40 nm)/NPB (50 nm)/*syn*-PyDTI or *anti*-PyDTI (20 nm)/TPBI (40 nm)/LiF (0.5 nm)/Al (120 nm). The electroluminescent properties are summarized in Figure 4 and Table S4. The turn-on voltages were measured as 2.8 V for both devices, suggesting that the barriers for carrier injection were quite low. They both exhibited green emissions, with peaks centered at 500 nm for *syn*-PyDTI and 508 nm for *anti*-PyDTI, that were very similar to their emission spectra in the film state. The maximum current efficiency ($\eta_{c.max}$) and power efficiency ($\eta_{p.max}$) of *syn*-PyDTI were as high as 11.42 cd A^{-1} and 10.39 lm W^{-1}, respectively, which were rarely obtained in pyrene-based OLEDs.[27] Even when the brightness reached 10000 cd m^{-2}, the $\eta_{c.max}$ remained nearly unchanged and displayed a very low roll-off in efficiency. Comparatively, the device using *anti*-PyDTI as the active layer showed a moderate performance with a $\eta_{c.max}$ of 8.12 cd A^{-1} and a $\eta_{p.max}$ of 6.71 lm W^{-1}. The higher efficiency and better device performance of *syn*-PyDTI make it the better candidate for OLED applications.

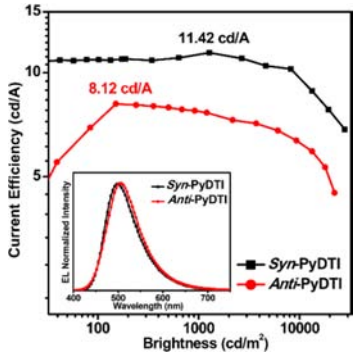

Figure 4. Current efficiency versus brightness curves for *syn*-PyDTI and *anti*-PyDTI. Inset: Electroluminescence (EL) spectra for *syn*-PyDTI and *anti*-PyDTI measured at 9 V.

In summary, two structural isomers with a pyrene−imidazole structure, *syn*-PyDTI and *anti*-PyDTI, were conveniently synthesized and successfully separated. When compared with *anti*-PyDTI, *syn*-PyDTI exhibits a 2-fold higher quantum efficiency as a crystal and 1.5-fold higher quantum efficiency as an evaporated amorphous film, although the two isomers possess the same apparent electronic structure. This observation reveals the dependence of molecular excited state properties derived from distinct structural symmetries. *Syn*-PyDTI also displays much better performance in OLEDs with a $\eta_{c.max}$ of 11.42 cd A^{-1} (8.12 cd A^{-1} for *anti*-PyDTI). Such findings are very relevant to OLED materials because precise separation is essential for enhanced device performance. The current work reports the establishment of stable imidazole-based isomers with very convenient accessibility and multifunctionality. We expect that the present strategy can provide a generic route toward novel and advanced structural isomers and that these materials may find practical applications in optoelectronics.

■ ASSOCIATED CONTENT

Supporting Information

The Supporting Information is available free of charge on the ACS Publications website at DOI: 10.1021/acs.orglett.5b02879.

Experimental procedures, DFT calculations, and characterization data (PDF)
X-ray crystal details for *syn*-PyDTI (CIF)
X-ray crystal details for *anti*-PyDTI (CIF)

■ AUTHOR INFORMATION

Corresponding Author

*E-mail: lup@jlu.edu.cn.

Notes

The authors declare no competing financial interest.

■ ACKNOWLEDGMENTS

This work was supported financially by the Ministry of Science and Technology of China (2013CB834801) and the National Science Foundation of China (21374038 and 91233113).

■ REFERENCES

(1) (a) Weissman, K. J. *Nat. Chem. Biol.* **2015**, *11*, 660. (b) Faulkner, A. D.; Kaner, R. A.; Abdallah, Q. M. A.; Clarkson, G.; Fox, D. J.;

DOI: 10.1021/acs.orglett.5b02879
Org. Lett. 2015, 17, 6138−6141

Gurnani, P.; Howson, S. E.; Phillips, R. M.; Roper, D. I.; Simpson, D. H.; Scott, P. *Nat. Chem.* **2014**, *6*, 797.
(2) Nakamura, K.; Greenwood, A.; Binder, L.; Bigio, E. H.; Denial, S.; Nicholson, L.; Zhou, X. Z.; Lu, K. P. *Cell* **2012**, *149*, 232.
(3) Moulton, B.; Zaworotko, M. J. *Chem. Rev.* **2001**, *101*, 1629.
(4) (a) Song, D. T.; Schmider, H.; Wang, S. N. *Org. Lett.* **2002**, *4*, 4049. (b) Wu, J. S.; Lin, C. T.; Wang, C. L.; Cheng, Y. J.; Hsu, C. S. *Chem. Mater.* **2012**, *24*, 2391.
(5) Chung, J. W.; You, Y.; Huh, H. S.; An, B. K.; Yoon, S. J.; Kim, S. H.; Lee, S. W.; Park, S. Y. *J. Am. Chem. Soc.* **2009**, *131*, 8163.
(6) (a) Zhang, S. Q.; Qiao, X. L.; Chen, Y.; Wang, Y. Y.; Edkins, R. M.; Liu, Z. Q.; Li, H. X.; Fang, Q. *Org. Lett.* **2014**, *16*, 342. (b) Hatano, S.; Horino, T.; Tokita, A.; Oshima, T.; Abe, J. *J. Am. Chem. Soc.* **2013**, *135*, 3164.
(7) Wang, Z. H.; Putta, A.; Mottishaw, J. D.; Wei, Q.; Wang, H.; Sun, H. *J. Phys. Chem. C* **2013**, *117*, 16759.
(8) Mamada, M.; Minamiki, T.; Katagiri, H.; Tokito, S. *Org. Lett.* **2012**, *14*, 4062.
(9) Lehnherr, D.; Hallani, R.; McDonald, R.; Anthony, J. E.; Tykwinski, R. R. *Org. Lett.* **2012**, *14*, 62.
(10) Yanai, N.; Mori, T.; Shinamura, S.; Osaka, I.; Takimiya, K. *Org. Lett.* **2014**, *16*, 240.
(11) Nakano, M.; Niimi, K.; Miyazaki, E.; Osaka, I.; Takimiya, K. *J. Org. Chem.* **2012**, *77*, 8099.
(12) Ma, B. B.; Peng, Y. X.; Zhao, P. C.; Huang, W. *Tetrahedron* **2015**, *71*, 3195.
(13) Gao, Z.; Cheng, G.; Shen, F. Z.; Zhang, S. T.; Zhang, Y. N.; Lu, P.; Ma, Y. G. *Laser Photonics Rev.* **2014**, *8*, 6.
(14) Zhu, M. R.; Yang, C. L. *Chem. Soc. Rev.* **2013**, *42*, 4963.
(15) Grimmett, M. R. In *Comprehensive Heterocyclic Chemistry, II*; Katritzky, A. R., Rees, C. W., et al., Eds.; Elsevier: Amsterdam, 1996; Vol.3, pp 77−220.
(16) Walba, H.; Isensee, R. W. *J. Org. Chem.* **1961**, *26*, 2789.
(17) Figueira-Duarte, T. M.; Müllen, K. *Chem. Rev.* **2011**, *111*, 7260.
(18) Moorthy, J. N.; Natarajan, P.; Venkatakrishnan, P.; Huang, D. F.; Chow, T. J. *Org. Lett.* **2007**, *9*, 5215.
(19) Figueira-Duarte, T. M.; Simon, S. C.; Wagner, M.; Druzhinin, S. I.; Zachariasse, K. A.; Müllen, K. *Angew. Chem., Int. Ed.* **2008**, *47*, 10175.
(20) Hu, J.; Zhang, D.; Harris, F. W. *J. Org. Chem.* **2005**, *70*, 707.
(21) Liu, Y. L.; Gao, Z.; Wang, Z. M.; Feng, C. F.; Shen, F. Z.; Lu, P.; Ma, Y. G. *Eur. J. Org. Chem.* **2013**, *32*, 7267.
(22) Winnik, F. M. *Chem. Rev.* **1993**, *93*, 587.
(23) Hong, Y. N.; Lam, J. W. Y.; Tang, B. Z. *Chem. Soc. Rev.* **2011**, *40*, 5361.
(24) Wang, J.; Mason, R.; VanDerveer, D.; Feng, K.; Bu, X. R. *J. Org. Chem.* **2003**, *68*, 5415. (b) Wang, J.; Dyers, L.; Mason, R.; Amoyaw, P.; Bu, X. R. *J. Org. Chem.* **2005**, *70*, 2353.
(25) Kastler, M.; Pisula, W.; Wasserfallen, D.; Pakula, T.; Müllen, K. *J. Am. Chem. Soc.* **2005**, *127*, 4286.
(26) (a) Liao, Y.; Bhattacharjee, S.; Firestone, K. A.; Eichinger, B. E.; Paranji, R.; Anderson, C. A.; Robinson, B. H.; Reid, P. J.; Dalton, L. R. *J. Am. Chem. Soc.* **2006**, *128*, 6847. (b) Lv, A.; Stolte, M.; Wűrthner, F. *Angew. Chem., Int. Ed.* **2015**, *54*, 10512.
(27) (a) Zhao, Z. J.; Chen, S. M.; Lam, J. W. Y.; Lu, P.; Zhong, Y. C.; Wong, K. S.; Kwok, H. S.; Tang, B. Z. *Chem. Commun.* **2010**, *46*, 2221. (b) Thomas, K. R. J.; Lin, J. T.; Tao, Y. T.; Ko, C. W. *Adv. Mater.* **2000**, *12*, 1949.

DOI: 10.1021/acs.orglett.5b02879
Org. Lett. 2015, 17, 6138−6141